RSC Advances

ROYAL SOCIETY OF CHEMISTRY

www.rsc.org/advances

Cite this: DOI: 10.1039/c0xx00000x

www.rsc.org/xxxxxx

ARTICLE TYPE

Highly Active Sustainable Ferrocenated Iron Oxide Nanocatalysts for the Decolorization of Methylene Blue

Atchaleeya Jinasan,[a,b] Thinnaphat Poonsawat,[a] Laksamee Chaicharoenwimolkul,[c] Soraya Pornsuwan[a] and Ekasith Somsook*[a]

Received (in XXX, XXX) XthXXXXXXXXX 20XX, Accepted Xth XXXXXXXXX 20XX
DOI: 10.1039/b000000x

Ferrocenated iron oxide nanoparticles were successfully synthesized in a basic condition. It was unexpected to discover the highly active sustainable nanocatalysts for the decolorization of methylene blue in the absence of light and hydrogen peroxide. Cyclopentadienyl radicals may be responsible for the production of active species for the decolorization of methylene blue. The nanocatalysts can be reactivated in sodium chloride solution and reused for several times.

The urbanization in many fast-growing developing countries leads to the increasing demand and shortage of clean water.[1] Therefore, new sustainable technologies are being developed to solve this problem. At present, innovative tools such as advanced oxidation processes[2] involving highly reactive oxygen species can be used for the treatment of wastewater. Fenton reaction[3] is a well-known reaction between Fe(II) and hydrogen peroxide to generate Fe(III), hydroxide and hydroxyl radical to eliminate pollutants. The key intermediates are hydroxyl radicals generated *in situ* in those processes. Dyes are basically represented as the pollutants.[4] Generally, excess hydrogen peroxide is required for Fenton reaction to generate active hydroxyl radicals for the decomposition of dyes.[5] However, it is not practical to use excess hydrogen peroxide for the real application.

Iron oxides are abundant, cheap and available almost everywhere on earth.[6] In the light of environmental concerns, it is sustainable to use iron oxide for the water treatment by adsorption process[7] and advanced oxidation process.[8] Iron oxide is usually inert and excess hydrogen peroxide is required for generating hydroxyl radicals for this application. Furthermore, iron oxide can be selectively separated out from the reaction by applying a magnetic field.[9]

Ferrocene ($(C_5H_5)_2Fe$ or Fc)[10] is a nonpolar molecule which is soluble in concentrated sulfuric acid to give a blue viscous solution of ferricinium or ferrocenium ($(C_5H_5)_2FeH^+$ or Fc^+).[10b, 11] The decomposition of Fc^+ undergoes very fast in neutral or basic aqueous solution.[12] It was observed that Fc^+ was transformed to orange precipitate at pH 9. Iron oxides are also formed as a result of this decomposition.[13] In addition, reactive oxygen species can be generated from the reaction of Fc^+ derivatives and dioxygen.[13-14] Herein, new ferrocenated iron oxide samples based on the coprecipitation of Fe(II) and Fe(III) and redox active species (Fc/Fc^+) in a basic condition were synthesized in which reactive oxygen species were expected to be produced for the decolorization of methylene blue under the aerobic condition. Ferrocenated compounds are termed for species deriving from ferrocene.

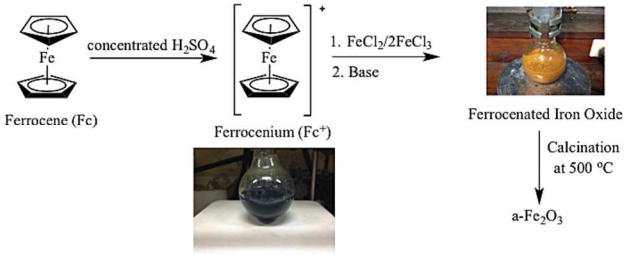

Scheme 1 Synthesis of ferrocenated iron oxide nanoparticles.

Table 1 Synthesis of iron oxide nanoparticles.

Sample	Fc^+:Fe(III):Fe(II)	Base	Temp. (°C)	Color
A1	3:2:1	NaOH	-	orange
A2	3:2:1	NaOH	500	red
A3	3:2:1	NH_4OH	-	orange
A4	3:2:1	NH_4OH	500	red
B1	5:2:1	NaOH	-	orange
B2	5:2:1	NaOH	500	red
B3	5:2:1	NH_4OH	-	orange
B4	5:2:1	NH_4OH	500	red
C1	0:2:1	NaOH	-	black
C2	0:2:1	NaOH	500	red brown
C3	0:2:1	NH_4OH	-	black
C4	0:2:1	NH_4OH	500	red brown

Different synthetic conditions were carried out as shown in Scheme 1 and Table 1 to study the phase transformation, morphology, magnetism, surface area, pore size, pore volume, surface state and composition, and catalytic activity of ferrocenated iron oxide nanoparticles. First, ferrocenium was simply prepared by reaction of ferrocene with 0.3 cm^3 of concentrated sulfuric acid and then a solution of $FeCl_2/FeCl_3$ was added into the ferrocenium solution. A NaOH or NH_4OH solution was slowly added dropwise the solution of $FeCl_2/FeCl_3$ with and without ferrocenium to adjust pH to 12 to obtain ferrocenated iron oxide samples (**A1**, **A3**, **B1**, **B3**) and iron oxide samples (**C1**, and **C3**), respectively. Then the prepared samples were calcined in a furnace at 500 °C under ambient atmosphere for 5 hours to produce calcined samples (**A2**, **A4**, **B2**, **B4**, **C2**, and **C4**). The color changes were observed after calcination with phase transformation from amorphous iron oxide to α-Fe_2O_3 crystalline[15] as indicated in XRD pattern (see *ESI*, Figure S1). The XRD results revealed the patterns of ferrocene in **A1**, **A3**, **B1**

and **B3**.

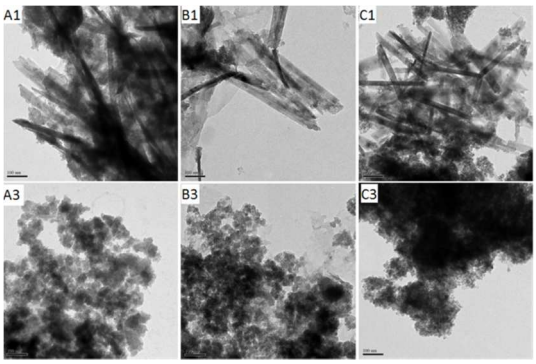

Figure 1 TEM images of ferrocenated iron oxide nanoparticles in ratio (**A1**) Fc^+/Fe(III)/Fe(II) = 3:2:1 with NaOH, (**A3**) Fc^+/Fe(III)/Fe(II) = 3:2:1 with NH_4OH, (**B1**) Fc^+/Fe(III)/Fe(II) = 5:2:1 with NaOH, (**B3**) Fc^+/Fe(III)/Fe(II) = 5:2:1 with NH_4OH, (**C1**) Fc^+/Fe(III)/Fe(II) = 0:2:1 with NaOH, and (**C3**) Fc^+/Fe(III)/Fe(II) = 0:2:1 with NH_4OH.

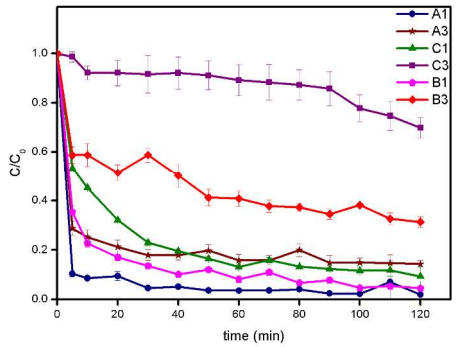

Figure 2 The decolorization of methylene blue catalyzed by ferrocenated iron oxide nanocatalysts before calcination under the aerobic condition and in the absence of hydrogen peroxide and light.

The morphology of ferrocenated iron oxide depends on both base type and the ratio of starting Fc^+ in iron oxide reaction. From Figure 1, the TEM images revealed that the morphology of ferrocenated iron oxide samples prepared in the presence of NaOH was nanofiber having the width and length around 20 and 300 nm, respectively. However, the TEM images of the ferrocenated iron oxide samples synthesized in the presence of NH_4OH revealed that many small particles were aggregated to form clusters like a sponge. The particles showed an average diameter of less than 10 nm. Furthermore, the presence of ferrocene in the coprecipitation reaction had effects on the morphology where the higher amount of ferrocene yielded the larger particle size. The iron oxide sample prepared without the addition of Fc^+ yielded smaller particles. In addition, the zeta potentials of ferrocenated iron oxide samples were negative on the surface (See *ESI*, Table S1).

The surface state and surface composition of the prepared nanoparticles can be determined by XPS (see *ESI*, Figure S2 and Table S2).[16] The C *1s* signal at 284.9 eV (C–C) was observed only in **A1**, **A3**, **B1** and **B3** samples and diminished after calcination in **A2** sample.[15b] The photoelectron spectra revealed the binding energy of Fe *2p* at 708 eV for the **A1**, **A3**, **B1** and **B3** samples with the pattern of ferrocene.[17] Furthermore, Fe^{3+} $2p_{3/2}$ were found at 710, 711, and 713 eV, respectively for all samples.[18] The FTIR spectra confirmed the formation of iron oxide at 475 and 560-580 cm^{-1} (see *ESI*, Figure S3).[19] TGA/DSC revealed that the composition percentage of ferrocene in **A1** samples was about 60% (see *ESI*, Figure S4 and Table S3). The magnetization curves of iron oxide nanoparticles were determined with vibrating sample magnetometer (VSM) (see *ESI*, Figure S5). Hysteresis curves of **A1** and **A3** samples were paramagnetic[20] and that of **C1** was superparamagnetic[21] with zero coercivities. Interestingly, the magnetism change was observed from paramagnetic to ferromagnetic[15b] after calcination of **A1** sample. EPR spectra of all samples before calcination were determined (see *ESI*, Figure S6) with a strong signal of *g*-value about 2.0. This *g*-value corresponds to iron species of iron oxide.[22] On the other hand, the calcined samples gave broaden signals of Fe(III) ion with *g*-value at 3.8[22] as confirmed by the XPS data. The BET analysis describing surface area, pore size and volume of ferrocenated iron oxide nanoparticles was summarized in Table S4 (see *ESI*). It is clearly shown that the surface area and pore volume of most iron oxide catalysts before calcination decreased significantly when compared with after calcination. Moreover, all prepared samples were mesoporous. Furthermore, the CHN analysis revealed the lower percentages of carbon and hydrogen in the calcined iron oxide samples (see *ESI*, Table S5). The composition of prepared ferrocenated iron samples (**A1**, **A3**, **B1**, **B3**) may contain ferrocene, iron oxide, and other organic species.

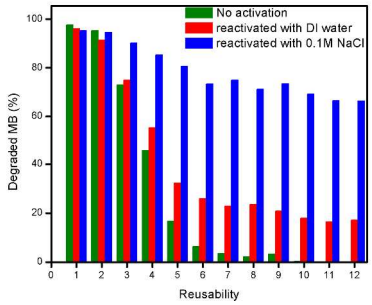

Figure 3 Reusability of **A1** catalyst with and without the reactivation by sodium chloride and de-ionized water.

The ferrocenated iron oxide nanocatalysts were applied in the decolorization of methylene blue that was monitored by spectrophotometry at λ_{max} = 662 nm. The catalytic decolorizations were carried out in a dark box without the addition of hydrogen peroxide. From Figure 2, **A1**, **B1**, and **C1** samples underwent rapid decolorization of methylene blue. The C/C_0 values decreased from 1 to less than 0.2 in 5 min for **A1**, 20 min for **B1**, and 40 min for **C1**, respectively. In the absence of ferrocene (**C1**), the decolorization of methylene blue was slower and the C/C_0 was constant at 0.13 even after 2 hours. It was found that the decolorization process was facilitated by ferrocene and the ratio of Fc^+:Fe(II) was maximized at 3:1. The NH_4OH systems (**A3**, **B3** and **C3**) generally exhibited slower decolorization. The ESI-MS analysis of the decolorization product in the presence of **A1** catalyst collecting at different times was very informative. Before decolorization, the signal of methylene blue was observed with m/z = 284 (see *ESI*, Figure S7).[23] At the longer time, this signal decreased and disappeared in 20 minutes along with the appearance of the decomposition products with m/z = 285, 301, and 317 (see *ESI*, Scheme S1). Other signals with m/z = 130 and 186 found at 5 minutes were assigned to dicyclopentadienyl cation and Fc^+, respectively. Several catalytic systems including ferrocene[24] for the decolorization or decomposition of methylene blue have been reported involving the addition of excess hydrogen peroxide.[5] Interestingly, it was found that the decolorization of methylene blue in the absence of hydrogen peroxide could be carried out in the presence of our catalysts even in the dark condition. In

addition, the **A1** catalyst was further used in the study of reusability as shown in Figure 3. In the first run, 98% of methylene blue was decolorized in 2 hours. However, the decolorization of methylene blue was dropped to 95, 73, and 3% for the 2nd, 3rd, and 9th runs, respectively. At the 10th run, the catalytic activity of **A1** catalyst was completely lost. To prolong the activity of nanocatalysts in the decolorization of methylene blue, the catalyst was reactivated with 0.1 mol/dm^3 sodium chloride and de-ionized water at the end of each run. Thus, the catalyst was active as seen in the high decolorization percentage of 95% and 96% for sodium chloride and de-ionized water at the first run and the catalyst was still active even at the 12th run. Here, sodium chloride played a role as exchanging ions to remove cationic methylene blue adsorbed on the catalysts. It was found that the concentrations of methylene blue eliminated from the catalysts were low at the 1st to 5th batch and higher at the 6th to 12th batch (see *ESI*, Figure S8). Two mechanisms may be attributed to the decolorization of methylene blue. At the first run, the methylene blue may be decomposed by active species from reaction of catalyst and dioxygen. After the first run, the reactive species may be lost due to leaching to the solution. However, the decolorization of methylene blue could proceed through the adsorption mechanism as the adsorbed species could be removed by sodium chloride.

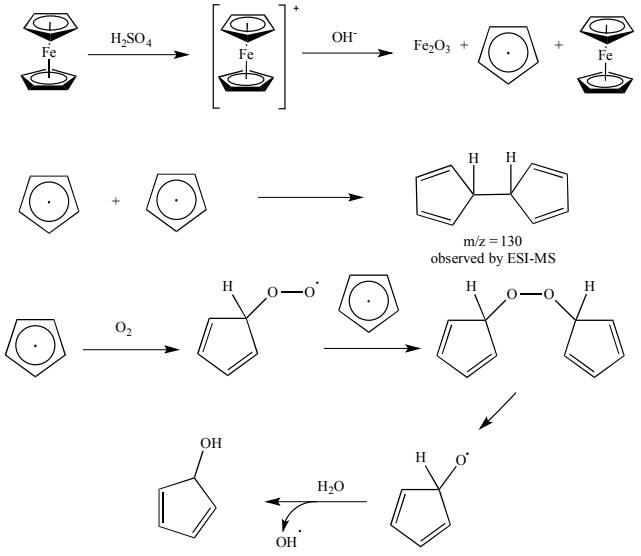

Scheme 2. Proposed mechanism of the demetallation of ferrocenium to generate cyclopentadienyl radicals and reactive oxygen species.

The detection of "short-lived" free radicals in iron oxide catalyst can be investigated with spin trapping technique.[25] EPR spectra of DMPO adducts in phosphate buffer and these simulation of adducts described the percentage of superoxide and hydroxyl adducts were shown in Figure S9. The percentage of superoxide adduct in fresh **A1** catalyst decreased significantly from 72% to 40% when these catalysts were reused in 12 times with 0.1 mol/dm^3 sodium chloride as shown in Table S6. The decolorization of methylene blue can be explained by the proposed mechanism of the demetallation of ferrocenium to produce "stable" cyclopentadienyl radical and then reactive oxygen species (ROS) as shown in Scheme 2. Free Fe(II), Fe(III), and iron oxide derived from ferrocene and the coprecipitation of Fe(II) and Fe(III) were not active enough to generate ROS in the system. In a separated experiment, the decolorization of methylene blue solution under an inert atmosphere was slower indicating that molecular oxygen was required to generate ROS and presumably the ROS was not generated at the starting of experiment until dissolving in the water (see *ESI*, Figure S10). Dicyclopentadienyl radical was derived from the dimerization of cyclopentadienyl radical as observed by ESI-MS at m/z=130.

In conclusions, ferrocenated iron oxide nanoparticles were successfully synthesized by coprecipitaion of Fc^+, Fe(II) and Fe(III) in a basic condition. The decolorization of methylene blue was carried out in the presence of these nanoparticles in the absence of light and hydrogen peroxide. These nanocatalysts can be regenerated to prolong the life of nanocatalysts in the presence of sodium chloride solution. This method can be used as a sustainable approach for the water treatment.

Experimental Section

Preparation of nanocatalysts

The coprecipitation of Fe(II), Fe(III), and ferrocenium ion was carried out at different ratio including different bases. The following procedure is for the preparation of **A1** or **A3** sample. Other ratios can be adjusted accordingly. Concentrated sulfuric acid (0.3 cm^3) was added to ferrocene (6.84 g, 36.75 mmol) and stirred for 2 minutes giving a blue viscous solution. Water (5 cm^3) was then added and stirred for 30 min. A solution of ferrous chloride tetrahydrate (1.55 g, 12.25 mmol) and ferric chloride hexahydrate (4.15 g, 25.6 mmol) in 80 cm^3 de-ionized water was then added into the ferrocenium solution and stirred for 1 hour. 8.35 mol/dm^3 NaOH or 4.83 mol/dm^3 NH_4OH solution was slowly added dropwise to adjust pH to 12 giving an orange precipitate. The mixture was then stirred for 2 hours. The orange precipitate was collected by centrifugation at 4500 rpm for 20 minutes. The product was purified by alternate washing with de-ionized water, collected by centrifugation for 6 times, and checked sulfate salt with dropwise de-ionized water after washing in $BaCl_2$ solution. The orange solid was then incubated at 80 °C for 24 hours giving 8.69 g product. The product may be further calcined at 500 °C for 5 hours to give **A2** sample.

The decolorization of methylene blue

The desired catalyst (0.100 g) was added into a solution of methylene blue (9.97×10^{-6} mol/dm^3, 100 cm^3). The reaction flask was wrapped with aluminium foil and kept in the dark box while stirring. At desired time, 3 cm^3 of the solution mixture was collected for analysis. The catalyst was separated from the mixture by centrifugation at 4500 rpm for 3 minutes. The clear supernatant was analyzed by UV-visible spectrophotometer and ESI-MS. To reuse of the catalyst, the separated resulting catalyst was then added a methylene blue solution (9.97×10^{-6} mol/dm^3, 100 cm^3) for the second run. The process was repeated as needed.

The reactivated catalyst

The catalyst was added a solution of the reactivator (100 cm^3) (0.1 mol/dm^3 sodium chloride and de-ionized water), stirred for 10 minutes, and separated by centrifugation at 4500 rpm for 3 minutes.

Instruments

The ferrocene-trapped iron oxide nanoparticles were characterized by X-ray powder diffraction (XRD). The XRD pattern was obtained on a Bruker D8 ADVANCE diffractometer with Cu-Kα radiation between 10° to 80°. The morphology images of nanoparticles were obtained by transmission electron microscopy (TEM) model JEOL JEM-2100 on copper grid covered by formvar. Fourier transform infrared spectroscopy (FTIR) was performed on Perkin Series to identify the functional groups in iron oxide. The UV-visible spectrophotometer was carried out on JASCO V-530 in range of 350-700 nm and scan speed of 1000 nm/min. Thermal analysis (DSC/TGA) was

performed on TA instruments SDT2960 Simultaneous using the heating rate at 20 °C/min from room temperature to 800 °C under nitrogen gas. Electrospray ionization (ESI) was carried out on microTOF, and positive ion mode. Electron paramagnetic resonance spectroscopy (EPR) was carried out on JEOL JES-RE2X operated at X-band microwave (8.8-9.6 GHz), magnetic field range of 3.1 T, cylindrical cavity resonator (TE_{011} mode), and program ES-PRIT. Vibrating sample magnetometer (VSM) was performed on electromagnet in model HV-4H, Hall probe-based gaussmeter on model Lakeshore 455, and field range up to ±9 kOe. X-ray photoelectron spectroscopy (XPS) was performed on Kratos Axis Ultra. Brunauer-Emmett-Teller (BET) was measured surface area, pore size and volume using a QuantachromeAutosorb Automated Gas Sorption System in nitrogen adsorption. The zeta potential technique was carried out with Zetasizer Nano-ZS model ZEN 3600. Elemental analyses were performed on a Perkin-Elmer series II CHNS/O Analyzer 2400.

Acknowledgements

The financial supports by the Biofuel development for Thailand fund through Center of Excellence for Innovation in Chemistry (PERCH-CIC), the Thailand Research Fund, and the Office of the Higher Education Commission-Mahidol University under the National Research University Initiative are acknowledged.

Notes and references

[a] *NANOCAST Laboratory, Center for Catalysis, Department of Chemistry and Center of Excellence for Innovation in Chemistry, Faculty of Science, Mahidol University, 272 Rama VI Rd., Ratchathewi, Bangkok 10400, Thailand. Fax: +(66)23547151; Tel: +(66)22015123; E-mail: ekasith.som@mahidol.ac.th*

[b] *The Materials Science and Engineering Program, Faculty of Science, Mahidol University, 272 Rama VI Rd., Ratchathewi, Bangkok 10400, Thailand*

[c] *Chemistry, Faculty of Science and Technology, Suratthani Rajabhat University, 272 Moo 9, Surat-Nasan Rd., Khuntale, Muang, Surat Thani 84100, Thailand.*

† Electronic Supplementary Information (ESI) available: synthesis and characterization data of the catalysts. See DOI: 10.1039/b000000x/

1. a. A. K. Biswas, Int. J. Water Resour. Dev., 2006, **22**, 183-197; bG. T. Daigger, Water Environ. Res., 2009, **81**, 809-823.
2. a. S. Malato, P. Fernández-Ibáñez, M. I. Maldonado, J. Blanco and W. Gernjak, Catal. Today, 2009, **147**, 1-59; b. M. N. Chong, B. Jin, C. W. K. Chow and C. Saint, Water Res., 2010, **44**, 2997-3027; cE. Neyens and J. Baeyens, J. Hazard. Mater., 2003, **98**, 33-50; dR. Andreozzi, V. Caprio, A. Insola and R. Marotta, Catal. Today, 1999, **53**, 51-59; eP. R. Gogate and A. B. Pandit, Adv. Environ. Res., 2004, **8**, 501-551.
3. H. J. H. Fenton, J. Chem. Soc., Trans., 1894, **65**, 899-910.
4. a. P. V. Nidheesh, R. Gandhimathi and S. T. Ramesh, Environ. Sci. Pollut. Res., 2013, **20**, 2099-2132; b. S. Rahim Pouran, A. A. Abdul Raman and W. M. A. Wan Daud, J. Clean. Prod., 2014, **64**, 24-35.
5. A. Dhakshinamoorthy, S. Navalon, M. Alvaro and H. Garcia, ChemSusChem, 2012, **5**, 46-64.
6. R. M. Cornell and U. Schwertmann, The Iron Oxides: Structure, Properties, Reactions, Occurences and Uses, Wiley VCH, 2003.
7. L. S. Zhong, J. S. Hu, H. P. Liang, A. M. Cao, W. G. Song and L. J. Wan, Adv. Mater., 2006, **18**, 2426-2431.
8. S. S. Lin and M. D. Gurol, Environ. Sci. Technol., 1998, **32**, 1417-1423.
9. C. T. Yavuz, J. T. Mayo, W. W. Yu, A. Prakash, J. C. Falkner, S. Yean, L. Cong, H. J. Shipley, A. Kan, M. Tomson, D. Natelson and V. L. Colvin, Science, 2006, **314**, 964-967.
10. a. T. J. Kealy and P. L. Pauson, Nature, 1951, **168**, 1039-1040; bG. Wilkinson, M. Rosenblum, M. C. Whiting and R. B. Woodward, J. Am. Chem. Soc., 1952, **74**, 2125-2126.
11. a. L. Chaicharoenwimolkul, S. Chairam, M. Namkajorn, A. Khamthip, C. Kamonsatikul, U. Tewasekson, S. Jindabot, W. Pon-On and E. Somsook, J. Appl. Polym. Sci., 2013, **130**, 1489-1497; b. L. Chaicharoenwimolkul, A. Munmai, S. Chairam, U. Tewasekson, S. Sapudom, Y. Lakliang and E. Somsook, Tetrahedron Lett., 2008, **49**, 7299-7302.
12. H. J. Hwang, J. R. Carey, E. T. Brower, A. J. Gengenbach, J. A. Abramite and Y. Lu, J. Am. Chem. Soc., 2005, **127**, 15356-15357.
13. a. G. Zotti, G. Schiavon, S. Zecchin and D. Favretto, J. Electroanal. Chem., 1998, **456**, 217-221; b. J. P. Hurvois and C. Moinet, J. Organomet. Chem., 2005, **690**, 1829-1839.
14. D. Osella, M. Ferrali, P. Zanello, F. Laschi, M. Fontani, C. Nervi and G. Cavigiolio, Inorg. Chim. Acta, 2000, **306**, 42-48.
15. a. A. Kay, I. Cesar and M. Grätzel, J. Am. Chem. Soc., 2006, **128**, 15714-15721; b. J. H. Bang and K. S. Suslick, J. Am. Chem. Soc., 2007, **129**, 2242-2243.
16. K. Sivula, R. Zboril, F. Le Formal, R. Robert, A. Weidenkaff, J. Tucek, J. Frydrych and M. Grätzel, J. Am. Chem. Soc., 2010, **132**, 7436-7444.
17. A. W. Taylor and P. Licence, ChemPhysChem, 2012, **13**, 1917-1926.
18. A. P. Grosvenor, B. A. Kobe, M. C. Biesinger and N. S. McIntyre, Surf. Interface Anal., 2004, **36**, 1564-1574.
19. H. Liu, Y. Wei, P. Li, Y. Zhang and Y. Sun, Mater. Chem. Phys., 2007, **102**, 1-6.
20. D. N. Srivastava, N. Perkas, A. Gedanken and I. Felner, J. Phys. Chem. B, 2002, **106**, 1878-1883.
21. R. Peng, W. Zhang, Q. Ran, C. Liang, L. Jing, S. Ye and Y. Xian, Langmuir, 2011, **27**, 2910-2916.
22. K. V. P. M. Shafi, A. Ulman, X. Yan, N.-L. Yang, C. Estournès, H. White and M. Rafailovich, Langmuir, 2001, **17**, 5093-5097.
23. A. C. Silva, R. M. Cepera, M. C. Pereira, D. Q. Lima, J. D. Fabris and L. C. A. Oliveira, Appl. Catal. B Environ., 2011, **107**, 237-244.
24. a. Q. Wang, S. Tian and P. Ning, Ind. Eng. Chem. Res., 2014, **53**, 643-649; b. Q. Wang, S. Tian and P. Ning, Ind. Eng. Chem. Res., 2014, **53**, 6334-6340.
25. M. A. Voinov, J. O. S. Pagán, E. Morrison, T. I. Smirnova and A. I. Smirnov, J. Am. Chem. Soc., 2011, **133**, 35-41.